12th International Conference on Structural Analysis of Historical Constructions
SAHC 2020
P. Roca, L. Pelà and C. Molins (Eds.)

NUMERICAL STUDY OF THE OUT-OF-PLANE BEHAVIOUR OF TIMBER RETROFITTED MASONRY PRISMS

JAMIU A. DAUDA[1*], LUIS C. SILVA[2], PAULO B. LOURENCO[2] AND ORNELLA IUORIO[1]

[1] School of Civil Engineering
University of Leeds
Woodhouse Lane, LS2 9JT, Leeds, UK
e-mail: cnjad@leeds.ac.uk (*corresponding author)
oiuorio@leeds.ac.uk

[2] Department of Civil Engineering
University of Minho
Azurém, P-4800-058 Guimarães, Portugal
e-mail: pbl@civil.uminho.pt

Keywords: ABAQUS, Flexure, Masonry, Numerical, OSB

Abstract. *The present study addresses the retrofitting of running-bond masonry walls through the application of oriented strand board (OSB) timber panels aiming to increase the masonry flexural strength and deformation capacity under out-of-plane actions. This paper presents the numerical analysis of masonry prisms to complement the information provided by the experimental campaign developed on flexural performances of timber retrofitted masonries. The numerical model represents the masonry components (brick and mortar) as a three-dimensional volume via volumetric finite elements, i.e. hexahedral 8-node linear brick elements with reduced integration and hourglass control. The nonlinear properties of the mortar joints and the brick units have been calibrated through information that resorts from experimental characterization tests. The numerical damage pattern and load-displacement capacity curve are compared with the experimental observations. A good agreement has been found and, therefore, the calibrated model can be employed in parametric studies, to further analyse the efficiency of the proposed timber masonry retrofit technique, and to more complex structural study cases.*

1 INTRODUCTION

Masonry structures show complex non-linear mechanical behaviour due to its heterogeneous and composite nature [1]. As such, computational numerical analysis of the mechanical behaviour of masonry structures is very complicated. Computational numerical analyses are useful to complement or as an alternative to experimental tests and may be used to predict the behaviour of structures to a given applied load. Numerical analyses are based on different theories such as finite element model (FEM), discrete/distinct element methods (DEM) or particle flow code (PFC), among others [2, 3 & 4]. FEM-based models are the most widely used due to the availability of many analysis software that operates based on this theory. Therefore, the numerical modelling strategy employed in this paper is based on FEM.

Many researchers who have previously worked on FE modelling of masonry structures [1, 2, 5 & 6] agreed that numerical modelling and analysis of masonry structures posed some of the greatest challenges to structural engineers. The main difficulty has been attributed to the presence of mortar joints which act as planes of weakness, discontinuity, and non-linearity. Besides, the existence of uncertainties in the material and geometrical properties is also another concern when modelling masonry structures [2, 3 & 7]. Despite, quite noteworthy advancements have been made on the application of numerical modelling in the study of mechanical behaviour of masonry structures, numerical analysis of masonry is still a significant area of research [8].

Therefore, this paper presents the numerical analysis on 665 x 215 x 102.5 mm masonry prism to complement the findings in [9]. Here, an accurate finite element model and analysis of the four-point bending test was developed to corroborate the interpretation of the test results obtained from the flexural bond strength test on masonry prism (MP). The main objective of this paper is to develop a concise and efficient nonlinear 3-D finite element analysis to simulate the damage and failure pattern of the masonry prism tested in the laboratory. The developed model was calibrated against the experimental results and analysed to evaluate the performance of the proposed OSB retrofit techniques of MP.

This paper is organised as follows. Section 1 entails the introductory comments as presented above. Section 2 describes the adopted modelling approach and the performed analysis. Section 3 compares the results of the numerical analysis with the experiments and discusses the model behaviour. Section 4 then encloses the paper with conclusions and recommendations.

2 MODELLING APPROACH AND ANALYSIS

Modelling of masonry structures is categorised into three different techniques shown in figure 1 [2]. The detailed micro-modelling is a material level model where masonry structure is considered as a three-phase material. Continuum elements are used to represent the masonry units and mortar joints while interface elements represent the unit–mortar interface. Meanwhile, for the simplified micro-modelling approach, the bricks are represented as fictitious expanded bricks by continuum elements. The mortar joint is then modelled as an interface with zero thickness. Macro-modelling, on the other hand, is a structural level modelling technique where the masonry components (unit and joint) are modelled as one phase material by smearing out masonry units, mortar and unit–mortar interface as a homogeneous continuum [2].

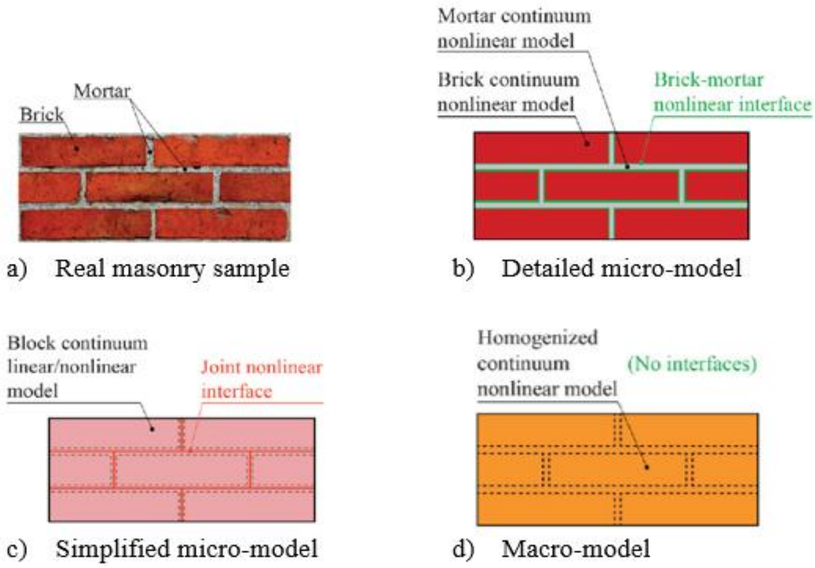

Figure 1: (a) Real masonry sample, (b) detailed micro-model, (c) simplified micro model, and (d) macro model

2.1 Model development and validation

Plain and retrofitted masonry prisms tested in [9] were chosen to verify the behavior prediction of the FE model. The goal is to provide a calibrated numerical model aiming a parametric analysis to evaluate the efficiency of the proposed timber masonry retrofit technique. The adopted model was based on the simplified micro-model technique described in figure 1c. The model was developed by following the steps in figure 2 and using the commercial software ABAQUS FEA. The four-point loading setup was numerically modelled following a detailed description for all the material components to achieve more accurate results. The full description of the numerical model, the assigned material properties and the adopted interactions are described as follows.

Two different models were created for the plain and retrofitted MP, and the models were labelled as MP00-NM and MPOSB-NM respectively. MP00-NM comprises of three components; brick unit, mortar and steel plate for load and support application. The brick unit (215 x 102.5 x 65 mm) and mortar joint (10 mm thick) were represented as three-dimensional deformable parts and meshed with a hexahedral 8-node linear brick, reduced integration, hourglass control (C3D8R) which has an improved convergence. The steel plate for load and support application (5 mm thick) was modelled using a 3-D discrete rigid element and discretised by rigid element R3D4 to represent a part that is stiffer (deformation negligible) than the masonry prism. For MPOSB-NM, two additional parts that are 18 mm thick OSB timber panel and the anchor rod were modelled as 3-D deformable parts and meshed with a hexahedral 8-node linear brick (C3D8R). The OSB timber panel and brick units were drilled at the connection locations as done in the experimental works [9, 10] to apply the retrofit to the MP.

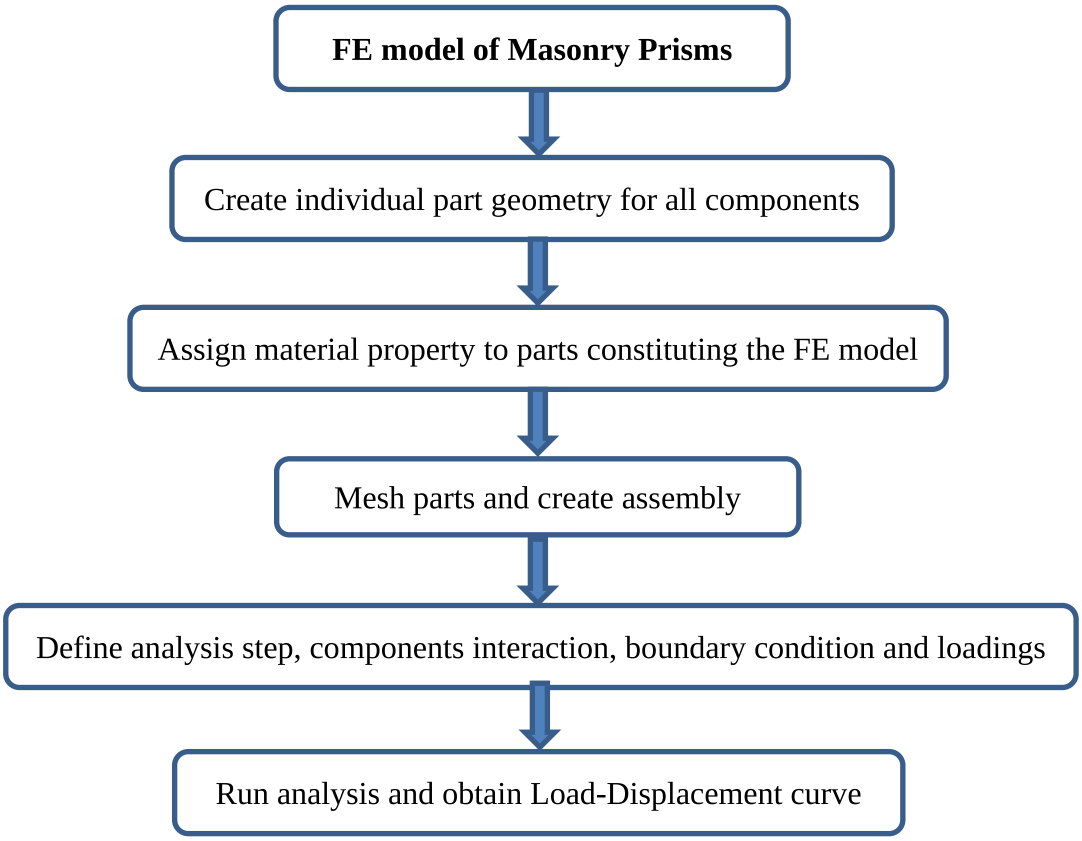

Figure 2: Steps for developing the FE model

The process to build the full model is such that an appropriate interaction and constraints between the model components are implemented to represent the relationship between them. Since the simplified micro modelling strategy is employed here, the brick-mortar bond interface was not specified separately, so the brick continuum and mortar continuum were merged as shown in figure 3a. In order to place the loading at the front face of the model, the surface of the steel plate was tied to the surface of the brick at the 3rd and 7th course using tie constraints (Fig 3b). Similarly, the steel plates were tied to the top and bottom brick at the back of the MP model as shown in figure 3c for the support application. The use of tie constraints ensured that the steel plate could not slip from the brick unit during analysis.

In the retrofitted model, the back-steel plates were tied to the back of the OSB (Fig. 3d). In addition to this, frictional, normal hard contact was specified between the surface of the OSB timber and MP model, as shown in figure 3e. For this analysis, the friction coefficient was taken as 0.5, which is a typical coefficient of friction between timber and brick.

For the anchor connection, the nodes on the surface of the brick around the connection holes were connected to the surface of the anchors using the default contact enforcement in ABAQUS (Fig. 3f). This connection ensures that there is a full adhesive bond between the anchor and the surface of the holes in MP. This kind of connection represents the retrofit system where the OSB timber panel is connected to the MP using adhesive anchor connection [9, 10].

More so, proper consideration of the applied boundary conditions in the numerical simulation was taken. The models were constrained to replicate what was done experimentally to enable a sound basis for comparison of results. In the created models, the nodes at the middle of the back-steel plate at the top of the MP were restrained in x and z-direction. Also, the plate at the bottom was restrained in all the three directions (x, y, z) at the middle nodes to replicate the support condition of the tested specimen (Fig. 4a).

The loads considered in this analysis are self-weight of the model and applied unit load in the out-of-plane direction at the third and seventh course of the model. This loading and support arrangement are a replica of the four-point bending test carried out in the laboratory. The out-of-plane load is applied as a unit uniform distributed load (UDL) on the steel plate tied to the front face of the model (Fig. 4b). The analysis is load control, similar to the test condition. The total load capacity of the model is measured as the load proportionality factor multiplied by the applied load in Newton (N).

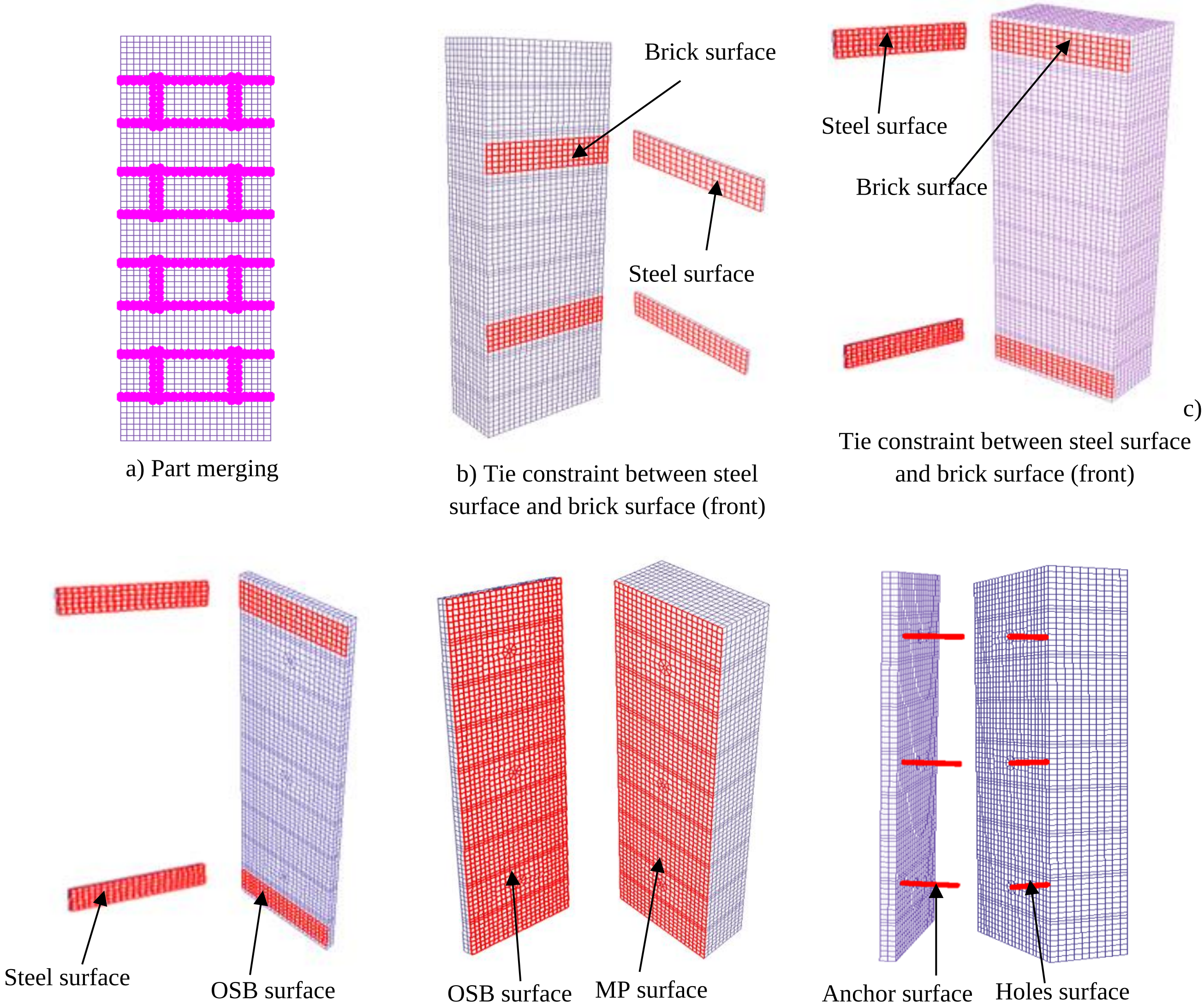

a) Part merging

b) Tie constraint between steel surface and brick surface (front)

c) Tie constraint between steel surface and brick surface (front)

d) Tie constraint between steel surface and OSB surface

e) Contact interaction between OSB surface and MP surface

f) Adhesive contact interaction between anchor and holes

Figure 3: Applied constraints and interaction in developing the FE model

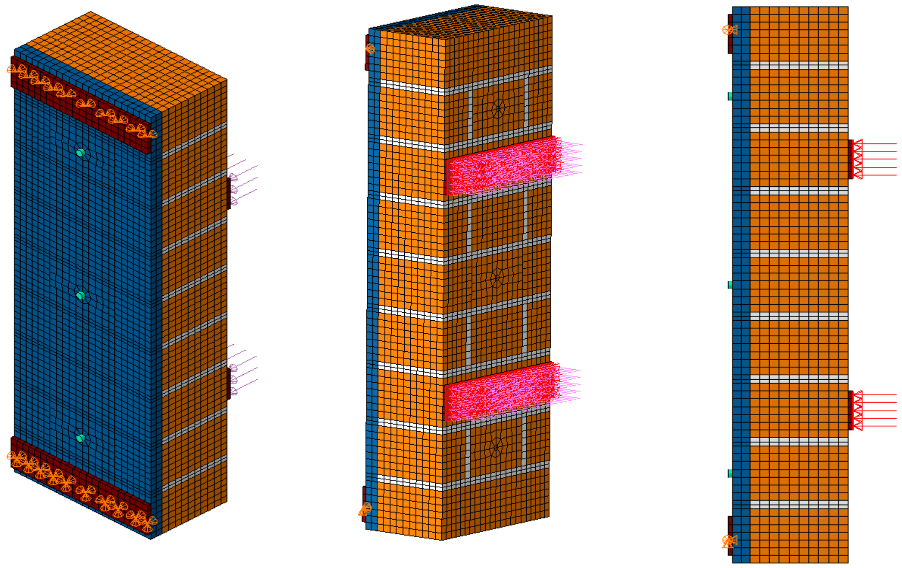

a) Boundary condition b) Loading c) Loading and BC (side view)

Figure 4: Applied boundary condition and load in the FE model

2.2 Input parameters

The assumed material parameters have been well described in previous work [11]. The Concrete Damage Plasticity (CDP) constitutive model was used to simulate the tensile and compressive non-linear behaviour of the brick unit and mortar. Also, the nonlinear response of the OSB timber panel is represented by an equivalent uniaxial stress-strain curve for both the compressive and tensile stress behaviour. The elastic properties used for the OSB were obtained from the manufacturer specification. The nonlinear behaviour, i.e. the stress-strain constitutive relation of the OSB was derived using existing guidelines [12]. The anchor rods were represented with a linear elastic behaviour, and the steel loading plates as rigid elements. Table 1 presents the abridged mechanical properties of the model components, the full properties, including the plastic-damaging behaviour parameters (Table 2) can be found in [11].

Table 1: Material properties (Elastic)

Properties	Brick	Mortar	OSB	Anchor
Mass density (γ) ton/mm^3	2.2e-9	2.17e-9	0.65e-9	7.85E-09
Young modulus (E) N/mm^2	32470	19850	3500	210000
Poisson ratio (μ)	0.26	0.2	0.24	0.3
Compressive strength (f_c) N/mm^2	87.91	7.1	6.6	
Tensile strength (f_t) N/mm^2	5.93	0.32	0.92	

Table 2: Material properties (Non-linear)

Brick				Mortar			
Compressive Behaviour		Tensile Behaviour		Compressive Behaviour		Tensile Behaviour	
Yield stress (N/mm^2)	Inelastic strain	Yield stress (N/mm^2)	Cracking strain	Yield stress (N/mm^2)	Inelastic strain	Yield stress (N/mm^2)	Cracking strain
26.37	0.00000	5.93	0.00000	1.79	0.00000	0.319	0.00000
68.00	0.00713	4.76	0.00017	3.13	0.00100	0.296	0.01096
78.10	0.01013	3.54	0.00037	4.997	0.00310	0.258	0.02303
84.80	0.01313	2.07	0.00077	5.825	0.00460	0.220	0.03179
87.91	0.01688	0.87	0.00167	6.521	0.00660	0.198	0.04086
72.26	0.02813	0.51	0.00247	6.970	0.00916	0.099	0.05156
36.79	0.03183	0.22	0.00437	7.100	0.01185	0.049	0.06996
19.36	0.03633			5.750	0.02360	0.025	0.09528
11.15	0.04113			3.483	0.03400	0.012	0.11836
				0.710	0.04800	0.006	0.34956

2.3 Analysis method

In this study, the full behaviour of masonry prism model under a continuous increase of load in the form of load-displacement was obtained through a quasi-static analysis. A load control type of analysis has been assumed since the tests were also load controlled. This analysis has been used to perform and validate the model with the obtained experimental data.

To represent softening, the Riks method (arc-length method) has been considered. This method is a robust method for nonlinear analysis, and it allows to properly reproduce the masonry nonlinear response. The adopted CDP model is based on a scalar-based damage model coupled with the plasticity one. Therefore, damage is given in terms of such scalar parameter and addressed separately in terms of compressive (*'damagec'*) and tensile (*'damaget'*) damage.

3 RESULTS AND DISCUSSION

In this section, the results from the numerical analysis are compared with the experimental ones and a brief discussion on the plain and retrofitted models is addressed. Figure 5 and 6 presents the failure of the non-retrofitted and retrofitted models alongside with the actual observed failure modes (tests designated as MP00 and MPOSB, respectively). The comparison shows that the failure of MP00 occurred in the bed joints within the loading span of the specimen. In the actual test, the total failure occurred in one bed joint, but the numerical model predicts a symmetrical failure on the middle span bed joints. In fact, and from a numerical standpoint, all the mortar joints present the same mechanical properties. In converse, the mechanical properties of the experimentally tested specimen have a spurious and inevitable variation that may be explained, for instance, by construction errors or by the existing dispersion of the material strength values. Hence, the symmetrical joints in the model will experience the same load, and thus the failure will be simultaneous. Whereas, the failure occurs in the weakest joint during the experimental test.

a)

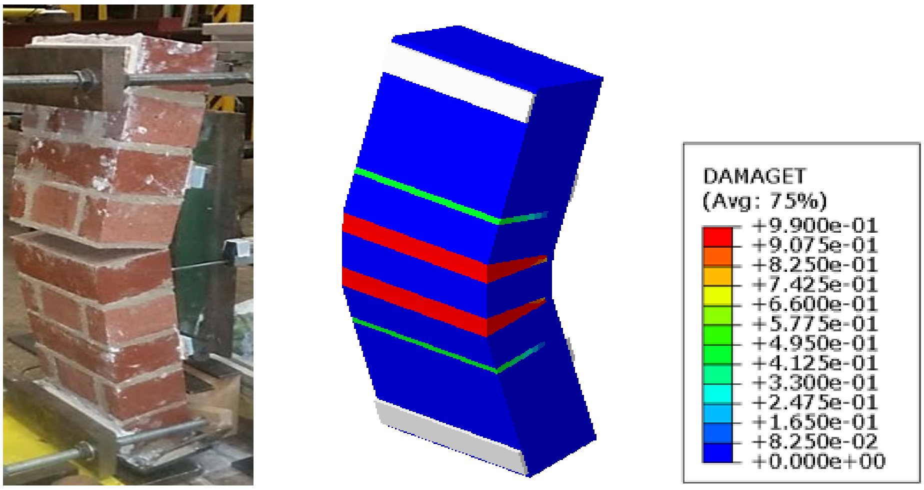

Figure 5: Failure pattern of MP00 (experimental and FE model)

In the case of the retrofitted specimens (MPOSB), the location and type of failure observed in the model output were compared with the experimental observation as highlighted. In the model, the global damage pattern shows all the areas where crack and failure happen occurred in all the tested specimens. References were made to two specimens highlighted for simplification (Fig. 6).

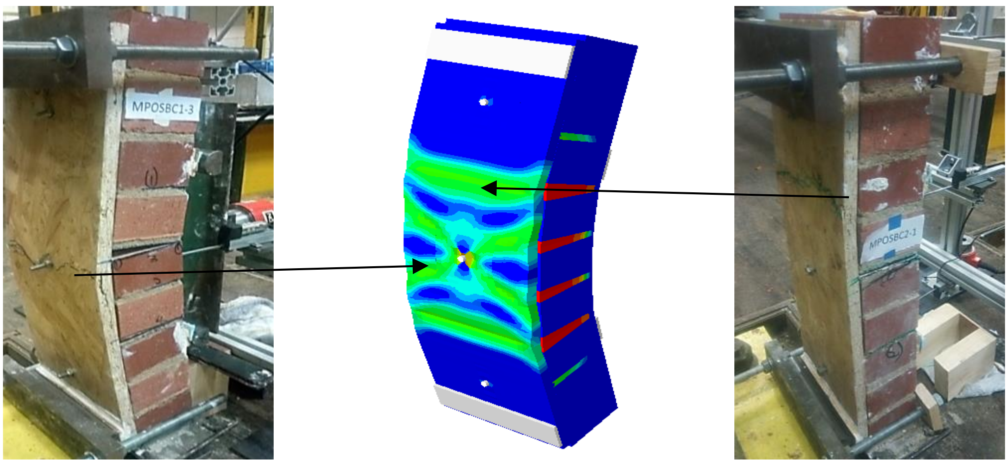

Figure 6: Failure pattern of MPOSB (experimental and FE model)

In terms of the load-displacement capacity curve comparison, Figure 7 shows that the numerical outputs resemble well with the experimental one. The numerical model is able to capture the experimental envelope and predicts the peak load and the corresponding failure to within less than 5% of the average results obtained from the test (Table 2). The curve shows the behaviour of the specimen at the initial elastic phase where the OSB and the masonry are bonded together before the crack initiated at an average load of 3640N for tested specimen and 3842N (5% variation) for the numerical model. This phase then followed by the complete failure of the joint in the masonry prism at an average load of 7982N and 8365N (4% variation) for the test and numerical specimen respectively. The final phase of the curve then presents a region where the masonry part has failed and the OSB is taking the load up to the failure of the OSB.

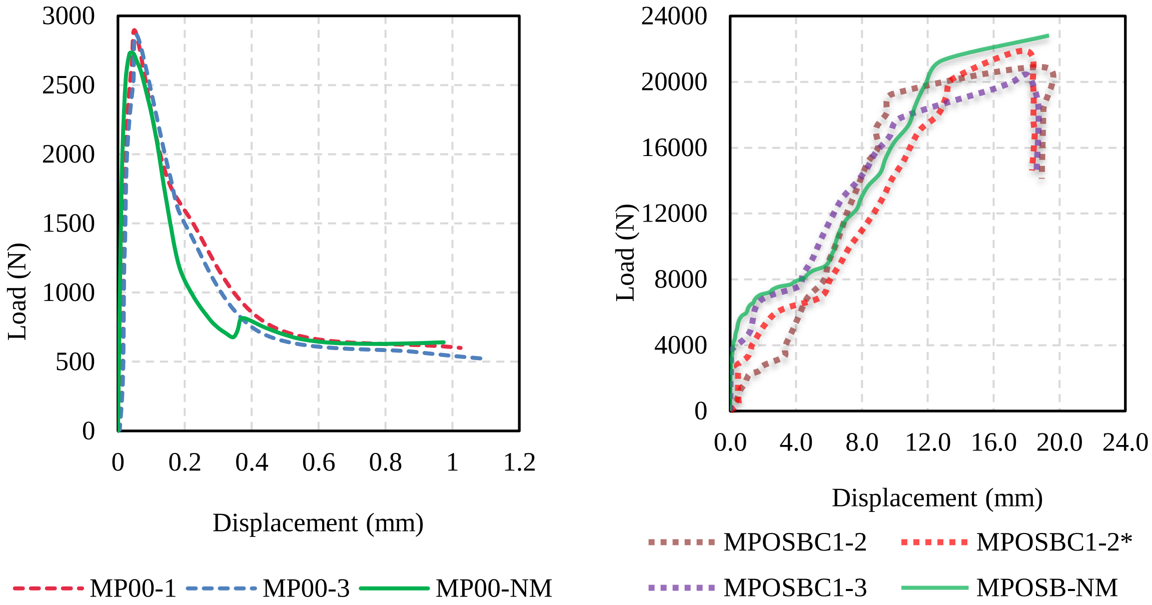

a) Plain masonry prism (MP00)

b) Retropfitted masonry prism (MPOSB)

Figure 7: Load-displacement curve (experimental and FE model)

Table 2: Comparison of model and test average results

Parameter	MPOO		MPOSB	
	Test	FE model	Test	FE model
Peak load (N)	2857	2723	21890	22820
Displacement (mm)	0.058	0.056	18.74	19.37

4 CONCLUSIONS

This paper presented part of the numerical study conducted to complement the results obtained from experimental tests on small-scale masonry prisms. A simplified detailed-micro model approach was employed to represent the four-point bending test and the advanced software ABAQUS was used. The mechanical properties for brick units and mortar joints have been calibrated from the performed experimental characterization as demonstrated in a previous work by the authors [11]. The Concrete Damage Plasticity (CDP) model available in ABAQUS has been assumed to describe the constitutive relation of the masonry and OSB timber panel. For the strengthened model, the connection between the masonry and the OSB panel is achieved through anchors whose behavior is assumed to be elastic.

Quasi-static analyses on the non-strengthened and strengthened masonry prisms were performed. Capacity curves were derived and represent the relationship among the continuous increasing load and maximum obtained displacement. The comparative analysis of the results with the experimental data confirms that the developed FE models can adequately capture the behaviour of both the plain and retrofitted walls, in terms of ultimate load capacity and damage failure patterns.

Generally, the numerical model predicted the peak load within a 5% deviation from the corresponding failure average load given by the experimental tests. This indicates that the model can be employed to carry out a parametric study to further investigate the performance of the proposed retrofit technique. Hence, parametric studies can be hereafter developed to assess the strengthening technique efficiency when applied to large-scale masonry walls and, as well, to optimize the required thickness of the OSB panels and the connection layout.

REFERENCES

[1] D'Altri, A., de Miranda, S., Castellazzi, G. and Sarhosis, V. (2018). *A 3D Detailed Micro-Model for the In-Plane and Out-Of-Plane Numerical Analysis of Masonry Panels*. Computers & Structures, 206, pp.18-30.

[2] Lourenco, P. (1996). *Computational Strategies for Masonry Structures*. PhD. Delft University of Technology.

[3] Asteris, P., Plevris, V., Sarhosis, V., Papaloizou, L., Mohebkhah, A., Komodromos, P. and Lemos, J. (2015). *Numerical Modeling of Historic Masonry Structures*. In: P. Asteris and V. Plevris, ed., Handbook of Research on Seismic Assessment and Rehabilitation of Historic Structures. IGI Global, pp.213-256.

[4] Zhang, S., Yang, D., Sheng, Y., Garrity, S. and Xu, L. (2017). *Numerical Modelling of FRP-Reinforced Masonry Walls under In-Plane Seismic Loading*. Construction and Building Materials, 134, pp.649-663.

[5] Silva L., Lourenço P. and Milani G. (2018) '*Derivation of the Out-Of-Plane Behaviour of Masonry through Homogenization Strategies: Micro-Scale Level*', Computer and Structures, 209, pp.30-43.

[6] CUR (1994). *Structural Masonry: An Experimental/Numerical Basis for Practical Design Rules (in Dutch).* Report 171, CUR, Gouda, Netherlands.

[7] Dogariu A. (2015) *Numerical Analysis of Steel Wire Mesh Seismic Retrofitting Techniques for Masonry Structures*. [Online] http://www.bipcons.ce.tuiasi.ro/Archive/519.pdf (Accessed 18 May 2017).

[8] Sacco E, Addessi D, Sab K. (2018). *New Trends in Mechanics of Masonry*. Meccanica 2018;53(7):1565–9.

[9] Dauda J., Iuorio O., and Lourenço P. (2019). *Experimental Study of Out-of-Plane Behavior of Timber Retrofitted Masonry Prisms.* In P.B.Dillon & F.S.Fonseca (Eds.), Proceedings of the 13th North American Masonry Conference, Salt Lake City, Utah (pp. 1100–1109).

[10] Dauda, J., Lourenço, P. and Iuorio, O. (in press). *Out-of-Plane Testing of Masonry Walls Retrofitted with Oriented Strand Board Timber Panels.* Proceedings of Institution of Civil-Engineer Structures and Building.

[11] Dauda, J., Iuorio, O. and Lourenço, P. (2020). *Numerical Analysis and Experimental Characterisation of Brick Masonry.* Int. Journal of Masonry Research and Innovation, Vol. 5 Issue: 3, pp.321–347, DOI: 10.1504/IJMRI.2020.10028163.

[12] Chen, G. and He, B. (2017). *Stress-strain Constitutive Relation of OSB under Axial Loading: An Experimental Investigation*. BioResources, 12(3).